Molecular Therapy
Oncolytics
Original Article

PET imaging and treatment of pancreatic cancer peritoneal carcinomatosis after subcutaneous intratumoral administration of a novel oncolytic virus, CF33-hNIS-antiPDL1

Zhifang Zhang,[1,4] Annie Yang,[1,4] Shyambabu Chaurasiya,[1] Anthony K. Park,[2] Sang-In Kim,[1] Jianming Lu,[1] Tove Olafsen,[3] Susanne G. Warner,[1,2] Yuman Fong,[1] and Yanghee Woo[1,2]

[1]Department of Surgery, City of Hope National Medical Center, 1500 E. Duarte Rd., Duarte, CA 91010, USA; [2]Cancer Immunotherapeutics Program, Beckman Research Institute, City of Hope National Medical Center, Duarte, CA 91010, USA; [3]Small Animal Imaging Core, City of Hope National Medical Center, Duarte, CA 91010, USA

Peritoneal carcinomatosis of gastrointestinal malignancies remains fatal. CF33-hNIS-antiPDL1, a chimeric orthopoxvirus expressing the human sodium iodide symporter (hNIS) and anti-human programmed death-ligand 1 antibody, has demonstrated robust preclinical activity against pancreatic adenocarcinoma (PDAC). We investigated the ability of CF33-hNIS-antiPDL1 to infect, help detect, and kill peritoneal tumors following intratumoral (i.t.) injection of subcutaneous (s.c.) tumors *in vivo*. Human PDAC AsPC-1-ffluc cells were inoculated in both the s.c. space and the peritoneal cavity of athymic mice. After successful tumor engraftment, s.c. tumors were injected with CF33-hNIS-antiPDL1 or PBS. We assessed the ability of CF33-hNIS-antiPDL1 to infect, replicate in, and allow the imaging of tumors at both sites (immunohistochemistry [IHC] and ^{124}I-based positron emission tomography/computed tomography [PET/CT] imaging), tumor burden (bioluminescence imaging), and animal survival. IHC staining for hNIS confirmed expression in s.c. and peritoneal tumors following virus treatment. Compared to the controls, CF33-hNIS-antiPDL1-treated mice showed significantly decreased s.c. and peritoneal tumor burden and improved survival ($p < 0.05$). Notably, 2 of 8 mice showed complete regression of disease. PET/CT avidity for ^{124}I uptake in s.c. and peritoneal tumors was visible starting at day 7 following the first i.t. dose of CF33-hNIS-antiPDL1. We show that CF33-hNIS-antiPDL1 can help detect and kill both s.c. and peritoneal tumors following s.c. i.t. treatment.

INTRODUCTION

Pancreatic adenocarcinoma (PDAC) is a fatal disease with few effective treatments. Over 400,000 pancreatic cancer diagnoses and deaths were reported in 2020 worldwide.[1] The majority of the patients present in the late stages of disease, when surgery is no longer beneficial and systemic therapy is palliative.[2] The first-line standard of care treatments for unresectable or metastatic PDAC include either FOLFIRINOX (5-FU, leucovorin, irinotecan, folic acid, and oxaliplatin) or gemcitabine plus nab-paclitaxel. Unfortunately, PDAC is remarkably treatment resistant, and the median survival for patients with unresectable disease is <8 months.[3–7]

To improve upon the 10% overall survival (OS) in PDAC, immunotherapy alone or combined with chemotherapy are under intense investigation.[8,9] Two promising groups of immunotherapeutic agents are oncolytic viruses (OVs) and immune checkpoint inhibitors (ICIs).[10] OVs have several key properties that make them strong anticancer agents. These include their inherent ability to selectively infect and replicate in cancer cells over normal human cells. Effective cancer cell infection and oncolysis can be achieved *in vivo* at safe doses of OV delivered via intravenous (i.v.), intratumoral (i.t.), and intraperitoneal (i.p.) injections with limited off-target viral infections. Large DNA OVs can serve as vectors of human transgene delivery to cancer cells that allow for cancer cell imaging and enhanced antitumor immunity. Following the approval of T-VEC (talimogene laherparepvec) as an OV therapy for advanced melanoma, there was a reemerging interest in OVs as anticancer agents for their ability to directly kill tumor cells and as vectors to locally deliver ICIs and recruit diverse immune cell subtypes into the tumor microenvironment (TME).[11] Furthermore, OVs with specific genetic modifications are being investigated for their ability to detect solid tumors at both local and distant sites after different routes of administration.

Human sodium iodide symporter (hNIS) is a transgene often inserted into the OV genome as a tumor-specific reporter gene.[12] hNIS is an integral plasma membrane glycoprotein that is mainly expressed in thyroid follicular cells that actively transports iodine

Received 24 August 2021; accepted 28 December 2021;
https://doi.org/10.1016/j.omto.2021.12.022.

[4]These authors contributed equally

Correspondence: Yanghee Woo, MD, FACS, Department of Surgery, City of Hope National Medical Center, 1500 E. Duarte Rd., Duarte, CA 91010, USA.
E-mail: yhwoo@coh.org

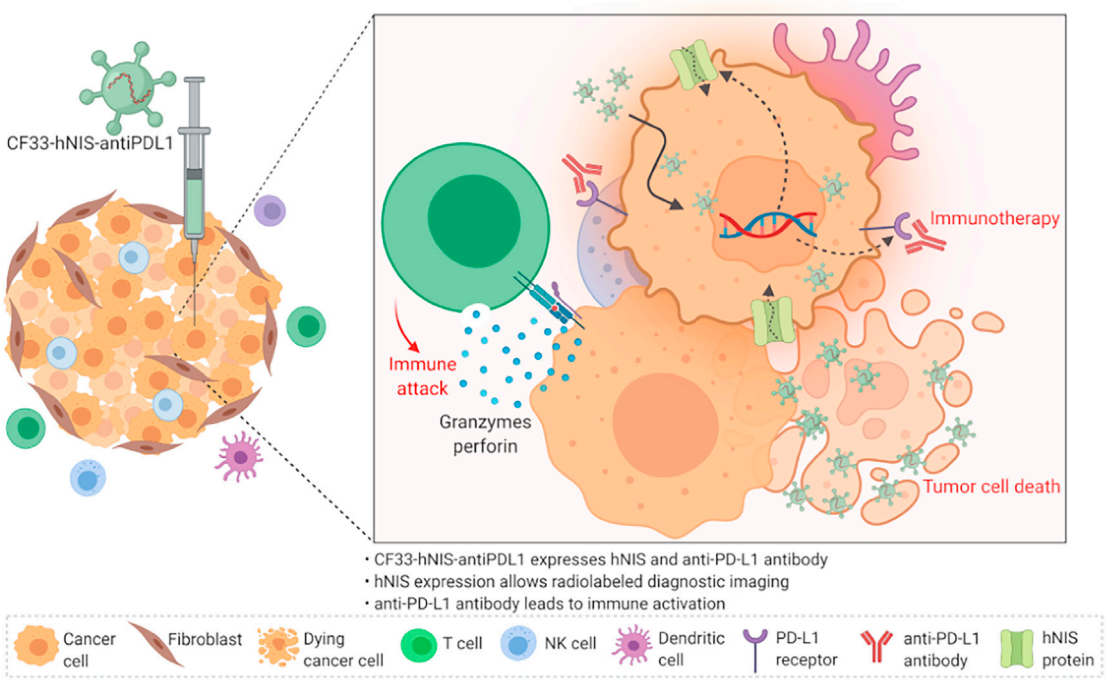

Figure 1. Schematic showing mechanism of action of CF33-hNIS-antiPDL1

In addition to targeted viral oncolysis of tumor cells, CF33-hNIS-antiPDL1 expresses the human sodium iodide symporter (hNIS) and the anti-PD-L1 antibody. hNIS allows radiolabeled diagnostic non-invasive imaging of virus-infected tumor cells, also killing tumor cells via radioiodine ablation. The anti-PD-L1 antibody blocks PD-1/PD-L1 interaction enhancing immune activation and eventually tumor cell death. Such a combination therapy converts an otherwise immunosuppressive tumor environment into an immunologically conducive environment to enhance antitumor efficacy.

(I^-) for thyroid hormone synthesis.[13] This transporting ability of hNIS allows for non-invasive imaging and treatment using radionucleotides in different cancers.[14–16] In this approach, tumor cells are directly killed by viral oncolysis as well as by the radiation emitted by the peripherally injected radioiodine. The synergy between hNIS and OVs has been shown to enhance therapeutic efficacy and monitoring of viral distribution via radioisotope uptake in both preclinical investigations and clinical trials.[17–22] In a Phase I trial, an oncolytic adenovirus expressing hNIS demonstrated safety in patients with prostate cancer and successful single-photon emission computed tomography (SPECT) imaging of viral propagation in prostate tumors.[23] Effective delivery of the hNIS transgene has also been reported using orthopoxviruses, which possess attractive immuno-oncolytic properties, such as a large cloning capacity, cytoplasmic replication, excellent human safety profiles, and short life cycles.[24,25]

We have engineered CF33, a chimeric orthopoxvirus, and its derivatives as an effective OV platform for the diagnosis and treatment of resistant solid tumors.[26,27] We previously demonstrated the safety and efficacy of CF33 in both xenograft and syngeneic mouse models of triple-negative breast cancer at doses several magnitudes lower than other OVs currently under investigation.[20,28] We designed CF33-hNIS-antiPDL1 (HOV3, Imugene, Sydney, Australia) expressing hNIS and the anti-programmed death-ligand 1 (anti-PD-L1) antibody for radiolabeled diagnostic imaging and targeted immunotherapy.[19,29] This third-generation CF33 variant has the potential to synergize OV therapy with iodine isotope ^{131}I treatment (or ^{124}I to image virus replication) and enhances local antitumor immunity by blocking PD-1/PD-L1 interaction (Figure 1). The safety and antitumor efficacy of CF33-hNIS variants was shown in breast, colon, liver, and pancreatic cancer, and the feasibility of real-time non-invasive imaging was demonstrated in a colorectal cancer model *in vivo*.[18–20,29] Moreover, CF33-hNIS-antiPDL1 kills human PDAC tumors *in vitro* and has greater efficacy against peritoneal disease when delivered intraperitoneally versus intravenously in mouse models of human PDAC.[19]

In this study, we investigated the ability of CF33-hNIS-antiPDL1 delivered into the subcutaneous (s.c.) tumor to detect and kill both s.c. tumors and peritoneal metastases. For the first time, we demonstrated ^{124}I-based positron emission tomography/computed tomography (PET/CT) imaging and the direct oncolytic efficacy of CF33-hNIS-antiPDL1 in an immunocompromised mouse model with s.c. and peritoneal PDAC tumors. Our results highlight both the diagnostic capacity of CF33-hNIS-antiPDL1 by radiolabeled imaging and the therapeutic benefit of locally delivered CF33-hNIS-antiPDL1 by the direct oncolysis of peritoneal metastases. This study was approved by the City of Hope's Institutional Animal Care and Use Committee (COH IACUC no. 15003).

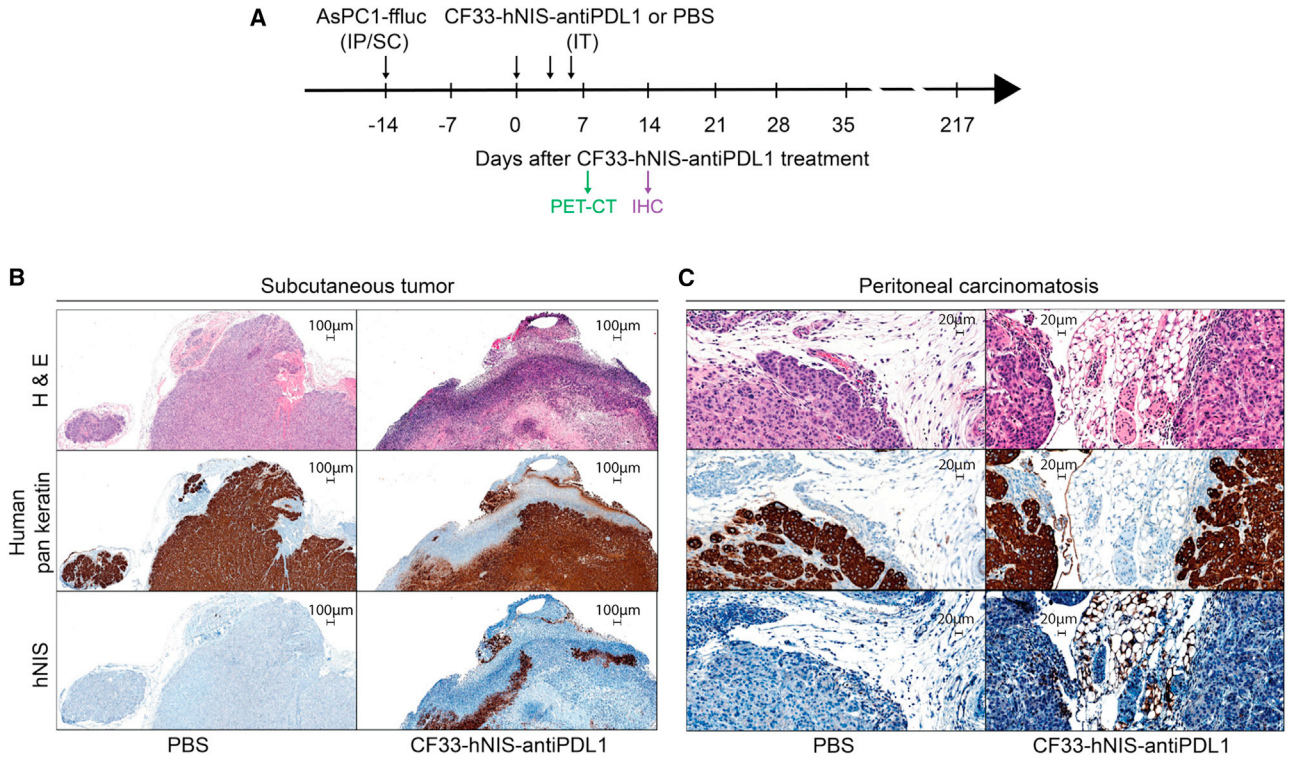

Figure 2. Immunohistochemical staining of subcutaneous (s.c.) tumors and peritoneal carcinomatosis (PC)

(A) Timeline showing s.c. and intraperitoneal (i.p.) inoculation of AsPC-1-ffluc cells (5×10^6 cells) in nude mice (−2 weeks). Treatment i.t. with CF33-hNIS-antiPDL1 or PBS (0 days), bioluminescence imaging time points (217 days), PET/CT image (green), and immunohistochemistry (IHC, purple) are shown. Nude mice were injected with CF33-hNIS-antiPDL1 or PBS 3 times (days 0, 3, and 5 at a dose of 3×10^5 pfu in 50 μL PBS). (B) Subcutaneous tumor nodules, in which CF33-hNIS-antiPDL1 or PBS were directly injected for 14 days, were harvested and stained with H&E to show cell structure (row 1). Anti-human pan-keratin antibody staining was performed to distinguish human tumor cells from mouse tissue (row 2). Anti-human hNIS staining verified virus-encoded human hNIS expression (row 3) (4× using Ventana Viewer Imaging software; scale bar, 100 μm). (C) A total of 14 days after i.t. injection of CF33-hNIS-antiPDL1 or PBS into the s.c. tumor, PCs were harvested and stained with H&E to show cell structure (row 1). Anti-human pan-keratin antibody staining was performed to distinguish human tumor cells with mouse tissue (row 2). Anti-human hNIS staining verified virus-encoded human hNIS expression (row 3) (20× using Ventana Viewer Imaging software; scale bar, 20 μm).

RESULTS

CF33-hNIS-antiPDL1 replicates in locally injected and distally located tumors to express functional hNIS protein

We used an aggressive xenograft model of PDAC with both s.c. tumor and peritoneal carcinomatosis (PC) that is fatal within 4–7 weeks to evaluate the ability of CF33-hNIS-antiPDL1 administered into the s.c. tumor to detect and kill both s.c. tumors and peritoneal metastases. After the establishment of s.c. tumors (~100 mm^3) and PC, mice were treated with either CF33-hNIS-antiPDL1 or PBS via i.t. delivery of s.c. tumors alone on days 0, 3, and 5 for a total of 3 times (Figure 2A). We observed a significant difference in bioluminescence imaging between the PBS group and the virus-treated group at day 14 post-injection and hence chose this time point to confirm virus replication in tumors. We harvested both s.c. and peritoneal tumors 14 days after treatment. We performed hematoxylin & eosin (H&E) to confirm the presence of tumor cells and human pan-keratin staining to distinguish human AsPC-1 tumor cells from the surrounding mouse tissue. CF33-hNIS-antiPDL1-injected s.c. tumors showed strong hNIS protein expression both inside and on the periphery compared to PBS-treated tumors (Figure 2B). In the peritoneum, we observed hNIS staining toward the edges of the tumor (Figure 2C). These results demonstrate that CF33-hNIS-antiPDL1 can successfully infect and replicate in both the locally injected and distally located tumors to express the hNIS protein.

^{124}I PET/CT imaging detects CF33-hNIS-antiPDL1 infection in PDAC tumors *in vivo*

We have previously shown that the human pancreatic cancer cell lines AsPC-1 and BxPC-3 express cell surface hNIS protein when infected with CF33-hNIS-antiPDL1.[29] Thus, ^{124}I can be used to detect CF33-hNIS-antiPDL1 replication in infected tumors *in vivo* and monitor oncolytic efficacy. We performed ^{124}I PET/CT imaging to test the functionality of virus-expressed hNIS to trace virus replication in tumors. CF33-hNIS-antiPDL1-infected s.c. tumor cells demonstrated strong ^{124}I signaling starting at day 7 and corresponded to the bioluminescence signaling of tumor burden (Figure 3).

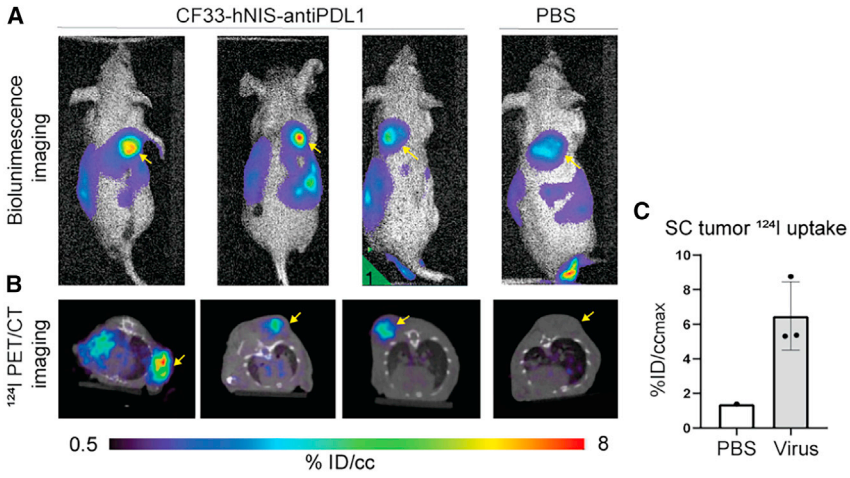

Figure 3. Imaging of CF33-hNIS-antiPDL1-infected AsPC-1-ffluc cells in s.c. tumors

On day 7 of i.t. CF33-hNIS-antiPDL1 administration, (A) bioluminescence imaging showing s.c. tumor burden and location (yellow arrows), and (B and C) ^{124}I PET/CT imaging showing hNIS signaling indicative of virus replication in the tumor following i.v. injection of 200 mCi ^{124}I for 2 h.

In the peritoneum, ^{124}I signaling was observed in all 3 CF33-hNIS-antiPDL1-treated mice (2 moderate and 1 weak signaling) compared to the control group at day 7 (Figure 4). Unlike the strong ^{124}I signaling that colocalized with the bioluminescence of s.c. tumors, ^{124}I signaling within the peritoneum was much weaker than the corresponding bioluminescence signaling (Figure 4). These results suggest that with i.t. treatment in s.c. tumors, CF33-hNIS-antiPDL1 can be delivered into the peritoneal cavity and replicates in PC, but they may need additional time and higher dosing to infect all of the peritoneal tumor cells.

Intratumoral CF33-hNIS-antiPDL1 administration decreases s.c. and peritoneal tumor burden

Next, we performed serial bioluminescence imaging to observe the efficacy of CF33-hNIS-antiPDL1 treatment on both the i.t.-injected s.c. tumors and the distally located PC. On day 7 after treatment, no difference in the s.c. tumor burden was observed between CF33-hNIS-antiPDL1-treated versus the control group. By day 14, the CF33-hNIS-antiPDL1-treated group showed significantly lower s.c. tumor burden compared to the control group ($p < 0.05$; Figure 5).

We observed a continued decrease in the peritoneal tumor burden in the CF33-hNIS-antiPDL1-treated group throughout sequential imaging of the animals. In contrast, the unchecked tumor growth in the control group led to the death of all of the animals. As measured by bioluminescence imaging, the greatest difference in the peritoneal tumor burden between the 2 groups was demonstrated at day 14 ($p < 0.05$; Figure 6). Six surviving mice in the CF33-hNIS-antiPDL1-treated group showed further decreased peritoneal tumor burden at 28 days compared to 14 days, as well as to the only surviving mouse in the control group. By day 217, the 2 surviving mice in the CF33-hNIS-antiPDL1-treated group showed complete remission of their PC (Figure 6). These data suggest that i.t. CF33-hNIS-antiPDL1 administration of s.c. tumors affects peritoneal tumors within 14 days, and this therapeutic efficacy leads to both complete remission and improved survival.

Intratumoral CF33-hNIS-antiPDL1 administration increases the OS of mice bearing AsPC-1-ffluc xenografts with peritoneal tumors

Lastly, we studied the effect of i.t. CF33-hNIS-antiPDL1 administration on the OS of these mice. All of the mice in the PBS group (n = 4) died between days 21 and 47, with a median survival of 35 days (Figure 7). In the CF33-hNIS-antiPDL1-treated group, 2 of 8 mice showed complete tumor regression of s.c. and peritoneal tumors,

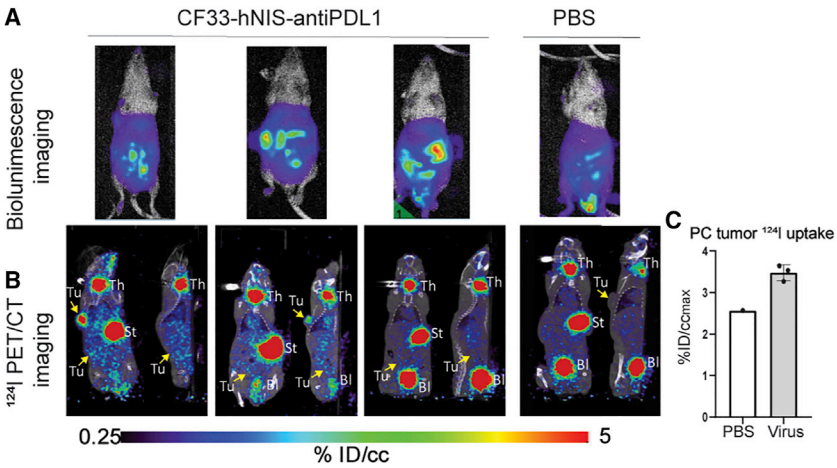

Figure 4. Imaging in PC after s.c. i.t. CF33-hNIS-antiPDL1 injection

On day 7 of i.t. CF33-hNIS-antiPDL1 administration, (A) bioluminescence imaging showing peritoneal tumor burden and location, and (B and C) ^{124}I PET/CT imaging showing hNIS signaling (yellow arrows) indicative of virus replication in peritoneal tumors following i.v. injection of 200 mCi ^{124}I for 2 h. Tu, tumor; Th, thyroid; St, stomach; Bl, bladder.

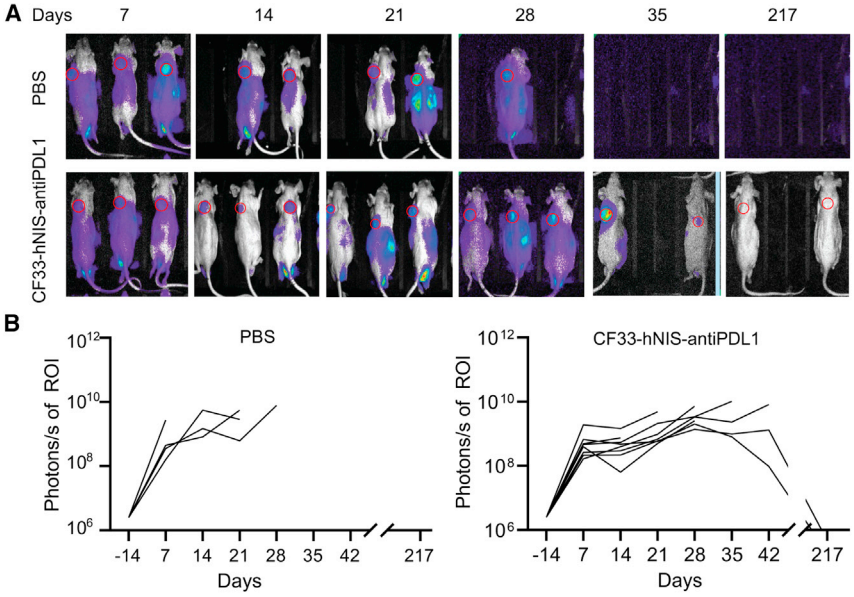

Figure 5. Bioluminescence imaging of s.c. tumors after i.t. CF33-hNIS-antiPDL1 injection

(A) Bioluminescence images of s.c. tumors from 3 representative mice per treatment group are shown at multiple time points between days 7 and 217 after treatment. The number above the images indicates the days after injection of PBS (n = 4) or CF33-hNIS-antiPDL1 (n = 8). Red circles indicate the area of imaging. (B) Graph showing s.c. tumor burden of PBS- and CF33-hNIS-antiPDL1-treated groups over days ($p < 0.05$ for day 14).

with significantly improved OS compared to the PBS group (Figure 7; $p < 0.05$). The weekly body weight and clinical status of mice are shown in Table 1. These results suggest that CF33-hNIS-antiPDL1 infection and replication in the s.c. tumors are robust and that i.t. treatment can lead to the infection and elimination of peritoneal tumors located distant from the site of injection to improve survival.

DISCUSSION

CF33-hNIS-antiPDL1 is a third-generation replication-competent orthopoxvirus chimera engineered for immuno-oncolytic therapy of otherwise treatment-resistant tumors. We demonstrated for the first time the oncolytic and imaging capabilities of CF33-hNIS-antiPDL1 following i.t. administration of the s.c. tumors to detect both the locally injected tumor and the peritoneal tumors distant from the injection site. The mouse model used in this study provides rapidly progressive tumors in the peritoneum that lead to jaundice, ascites, cachexia, and death within 4–7 weeks of tumor inoculation.[19] Here, we showed that 3 low doses of i.t. CF33-hNIS-antiPDL1 into the s.c. tumor resulted in infection, replication, and expression of the hNIS transgene in both the injected s.c. tumors and distantly located peritoneal tumors. This allowed for the successful imaging of the infected tumors by ^{124}I PET/CT. Repeated low doses of CF33-hNIS-antiPDL1 decreased the tumor burden at both sites, prevented complications of PC, and improved survival compared to the control animals. Most notably, CF33-hNIS-antiPDL1 completely eradicated both the injected s.c. tumors and peritoneal metastases in 2 of 8 mice.

We have previously demonstrated the robust replication and oncolytic potential of CF33-hNIS-antiPDL1 against human PDAC cell lines in a dose-dependent manner starting at an MOI of 0.01.[19,29] We have also confirmed its ability for transgene expression of hNIS and anti-PD-L1 proteins *in vivo*.[19,29] The effectiveness of OVs at different tumor sites varies with the route of treatment. To better understand the ability of CF33-hNIS-antiPDL1 to treat both primary and distant diseases, we have previously shown the efficacy of i.v. and i.p. routes of administration.[19] We have now evaluated the effectiveness of i.t. delivery.

In general, i.t. delivery ensures the accurate delivery of OVs into the tumor, minimizing adverse off-target effects.[30] Injection i.v. is a common OV therapy route that provides the advantages of clinical convenience at the time of patient treatment. However, in i.v. delivery, physiological blood-brain and blood-peritoneal barriers and OV elimination by the immune system prevent an optimal antitumor response.[30] OV therapy i.p. has the advantages of high intraabdominal volume and peritoneal-blood barrier for potentially higher dosing with less systemic toxicity. Moreover, due to the large peritoneal surface area, i.p.-injected drugs can be absorbed relatively faster into the bloodstream, and this route is an ideal choice for targeting tumors in the abdominal cavity. In contrast to the cytotoxic drugs for which the dose is fixed at the time of injection, CF33-hNIS-antiPDL1, like other replication-competent viruses, can have magnified oncolytic effects due to its ability to infect and replicate in cancer cells.

As expected, the delivery route of CF33-hNIS-antiPDL1 therapy had differing effects on the primary and peritoneal sites of the disease. In our previous study, while i.p. injection of CF33-hNIS-antiPDL1 effectively eliminated peritoneal disease and prolonged mouse survival, neither i.p. nor i.v. injections had any effect in reducing the s.c. tumor burden.[19] In contrast, here, we observed that i.t. delivery shows superior effectiveness against both primary and peritoneal tumors with improved survival. The potential of CF33-hNIS-antiPDL1 to replicate after i.t. injection of the primary tumor may be greater than after i.v. or i.p. delivery, and it could provide sufficient virus to infect peritoneal tumors and exert its oncolytic activity. This must be considered when designing effective treatment strategies against multiple tumor sites such as PDAC with PC.

Furthermore, the clinical utility of CF33-hNIS-antiPDL1 is enhanced by its ability to infect tumor cells and express the human transgene hNIS for radiolabeled tumor-specific imaging. We previously showed that CF33-hNIS-antiPDL1-infected AsPC-1 cells express the hNIS protein at 360 min post-infection *in vitro*.[29] In this study, we further confirm

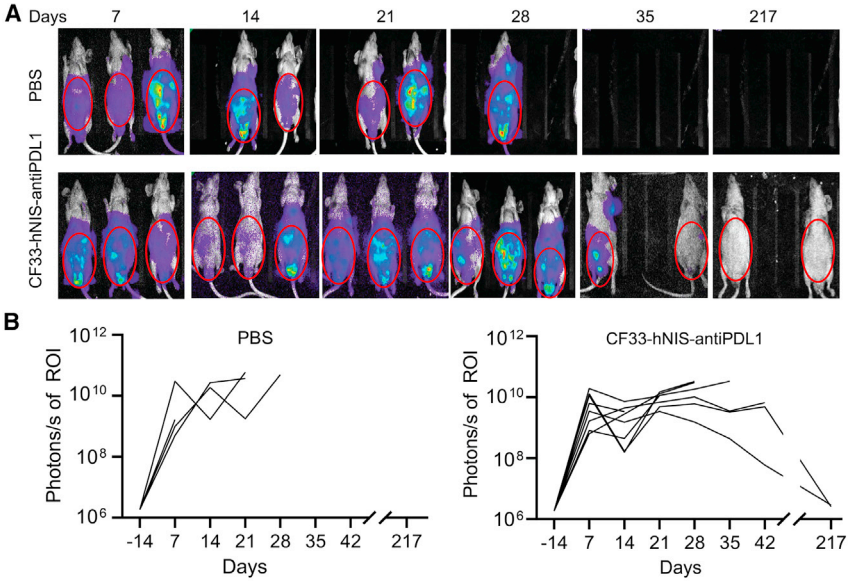

Figure 6. Bioluminescence imaging of peritoneal tumors after i.t. CF33-hNIS-antiPDL1 injection

(A) Bioluminescence images of PC from 3 representative mice per treatment group are shown at multiple time points between days 7 and 217 after treatment. The number above the image indicates the days after i.t. injection of PBS (n = 4) or CF33-hNIS-antiPDL1 (n = 8). Red circles indicate the area of imaging. (B) Graph showing PC tumor burden of PBS- and CF33-hNIS-antiPDL1-treated groups over days ($p < 0.05$ for days 14 and 21).

in vivo the uptake of the radioisotope by functional hNIS expressed in virus-infected cancer cells. Our findings demonstrate that CF33-hNIS-antiPDL1 retains its oncolytic capacity, detects distant infected tumors, and allows radiolabeled imaging of virus-infected cells via PET/CT imaging. Furthermore, functional hNIS provides the added potential for a synergistic therapeutic effect with radioiodine (^{131}I).

Our study has some limitations. For the ^{124}I PET/CT imaging of tumors, the expected physiologic hNIS expression also resulted in ^{124}I uptake in the thyroid and stomach, and isotope excretion was observed in the bladder beside tumor tissues. The ^{124}I signaling of PC is much weaker than s.c. tumors, and the interpretation of imaging can be complicated by physiologic ^{124}I uptake in the stomach and bladder. Another limitation is that the study was performed in an immunocompromised mouse model. This limited our ability to assess the potential T cell-associated immune effects. We chose not to use a syngeneic mouse model harboring mouse PDAC in this study because we sought to focus on evaluating the ability of CF33-hNIS-antiPDL1 to infect and express its transgene hNIS in human PDAC. CF33 and its variants, including CF33-hNIS-antiPDL1, have shown magnitudes higher tropism for human cancers when compared to murine cancer cells. Even at an MOI as high as 10, the virus elicits limited cytotoxicity against mouse cancer cells. In the future, we will use humanized immunocompetent PDAC models to evaluate the immune checkpoint inhibition function of CF33-hNIS-antiPDL1 and explore its collective efficacy with direct oncolysis and imaging/radiotherapy.

In summary, CF33-hNIS-antiPDL1 is a promising novel agent for the imaging and treatment of PDAC. Delivery i.t. of the virus eliminates both the s.c. tumor and peritoneal disease. As CF33-hNIS-antiPDL1 advances into clinical trials, radiolabeled imaging will be a valuable adjunctive tool to help evaluate the efficacy of various routes of OV delivery at different sites of disease.

MATERIALS AND METHODS

Reagents and virus

XenoLight D-luciferin-K + Salt Bioluminescent Substrate (catalog no. 122,799-5) was purchased from PerkinElmer (Waltham, MA, USA). Anti-human pan-keratin antibody (clone: AE1/AE3/PCK26, catalog no. 760-2135) was purchased from Roche Tissue Diagnostics (Rotkreuz, Switzerland); anti-human hNIS antibody (catalog no. HPA049055) was purchased from Sigma-Aldrich (St. Louis, MO, USA). Levothyroxine (catalog no. 1365000) was purchased from USP (Rockville, MD, USA). Iodine 124 (^{124}I) was ordered through the Radiopharmacy Core at the City of Hope National Medical Center. The CF33-hNIS-antiPDL1 virus, encoding both hNIS and the anti-PD-L1 single-chain antibody fragment (scFv), was generated as described previously.[19]

AsPC-1-ffluc cell lines

The human PDAC cell line AsPC-1 (pancreatic cancer cell line derived from metastatic ascites) was purchased from the American Type Culture Collection (ATCC; catalog no. CRL-1682, Manassas, VA, USA) and cultured in RPMI 1640 medium (Corning, catalog no. REF10-040-CM, Corning, NY, USA) supplemented with 10% FBS (catalog no. ES56811, Azer Scientific, Morgantown, PA, USA) and 1% antibiotic-antimycotic solution (Corning, catalog no. REF 30-004Cl). The cells were maintained in a humidified incubator at 37°C and 5% CO_2. The AsPC-1-ffluc cell line was established to stably encode firefly luciferase (ffluc) using lentiviral transduction as described before.[19] Briefly, AsPC-1 cells were incubated with polybrene (4 mg/mL, Sigma-Aldrich, catalog no. TR-1003-G) in RPMI 1640 containing 10% FBS and 1× antibiotic-antimycotic, and infected with lentivirus carrying ffluc cDNA under the control of the EF1a promoter. The expression of ffluc in AsPC-1 cells was confirmed, and single-cell clonal selection was performed by the limiting dilution method.[31]

In vivo mouse model of s.c. and peritoneal dissemination xenograft of human AsPC-1-ffluc cells

In vivo mouse studies were performed per the City of Hope Institutional Animal Care and Use Committee (IACUC)-approved protocol. Six-week-old Hsd:Athymic Nude-Foxn1nu female and male mice (Envigo) were purchased and acclimatized for 2 weeks. The unilateral

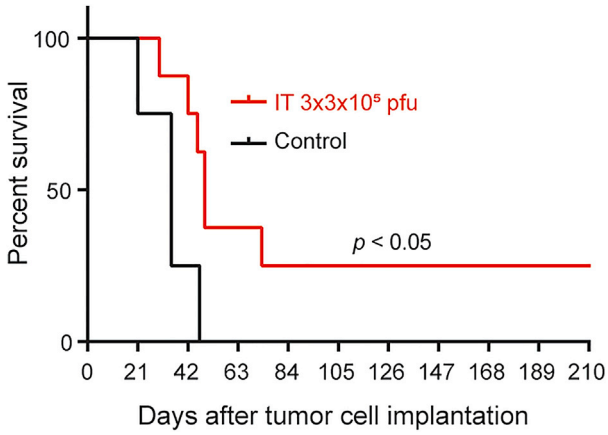

Figure 7. Survival analysis following i.t. CF33-hNIS-antiPDL1 administration in a s.c. and peritoneal dissemination xenograft model of human AsPC-1-ffluc cells

Kaplan-Meier survival analysis of the experiment. Mice were randomized into 2 groups 14 days after tumor inoculation. Control mice (n = 4) were treated i.t. with PBS 3 times (days 0, 3, and 5), and the CF33-hNIS-antiPDL1-treated group (n = 8) was i.t. injected with CF33-hNIS-antiPDL1 (3×10^5 pfu) 3 times (days 0, 3, and 5).

shoulder and peritoneal xenograft animal model was generated by s.c. and peritoneal injection of AsPC-1-ffluc cells to represent unresectable PDAC with PC and distinguish tumor burden at the time of imaging.[19] Briefly, injection of 5×10^6 AsPC-1-ffluc cells in a total volume of 100 μL PBS containing 50% Matrigel into the unilateral shoulder and the peritoneal cavity was performed for each mouse. When s.c. tumors reached 100 mm^3 in 14 days after inoculation, mice were divided into 2 groups: CF33-hNIS-antiPDL1 treatment group and PBS control group. Only the s.c. tumor of each mouse was i.t. injected with either CF33-hNIS-antiPDL1 (3×10^5 pfu in 50 μL PBS/each) for virus group (n = 14) and PBS for the control group (n = 10). These animals were evaluated for survival, PET/CT imaging, and IHC studies. Injection i.t. of the s.c. tumors were performed with virus (3×10^5 pfu/each) or PBS on days 0, 3, and 5 for a total of 3 times (Figure 2A).

IHC staining

Tumors were harvested 14 days after virus treatment, fixed with 10% formalin, embedded in paraffin, and cut into 5-mm-thick sections. Sections were stained with H&E, anti-human pan-keratin antibody (clone: AE1/AE3/PCK26, catalog no. 760-2135), and anti-human hNIS antibody (catalog no. HPA049055) was purchased from Sigma-Aldrich. Images were scanned using Ventana iScan HT and obtained using Ventana Image Viewer version 3.1.4 (Vantana Medical Systems, Oro Valley, AZ, USA).

Bioluminescence imaging

Each animal underwent bioluminescence imaging for luciferase activity of the tumor and was quantified to evaluate for tumor burden once per week. D-Luciferin solution was prepared by dissolving 1 g Xeno-Light D-luciferin-K + Salt Bioluminescent Substrate (PerkinElmer, catalog no. 122,799-5, Waltham, MA, USA) in 35 mL PBS at a 28.5-mg/mL concentration. Delivery i.p. (200 μL/mouse) was performed in all of the groups, and the mice were imaged using the Lago X optical imaging system (Spectral Instruments Imaging, Tucson, AZ, USA). Bioluminescence imaging was analyzed using Aura64 software (Spectral Instruments Imaging) and presented as photons/second for regions of interest.[19]

PET/CT imaging

In vivo mouse PET/CT imaging was performed per the City of Hope Radiation Safety Committee-approved protocol. On day 7 post-virus infection, mice were injected i.v. with a 200-μL volume of ~6 MBq free ^{124}I in the tail vein. For PET/CT imaging, mice were anesthetized with an i.p. injection of ketamine/xylazine, placed in a tube with a filter, and imaged while in the tube. Mice were imaged at 2 h post-injection. Static whole-body PET scans were acquired for 10 min, followed by 1-min CT scans using the small-animal GNEXT PET/CT imaging system (SOFIE, Dulles, VA, USA). The images were reconstructed by three-dimensional ordered subsets expectation-maximization (3D-OSEM) using the integrated GNEXT Acquisition Engine software. Co-registered PET/CT images were post-processed with Amide's a Medical Imaging Data Examiner (AMIDE) software.[32]

Statistics

Assay results were expressed as means ± SEMs, and paired or unpaired Student's t tests were used for comparisons. All p values are 2-sided. Data and Kaplan-Meier curves for survival were analyzed with GraphPad Prism software (version 7, GraphPad, San Diego, CA, USA). Comparison of survival was by log rank.

ACKNOWLEDGMENTS

Research reported in this publication included work performed in the Pathology Core, animal facility, Radiopharmacy Core, and Small Animal Imaging Core facilities supported by the National Cancer Institute of the National Institutes of Health under grant no. P30CA033572. The content is solely the responsibility of the authors and does not necessarily represent the official views of the National Institutes of Health. S.C. and S.-I.K. are supported through the generosity of Natalie & David Roberts. These authors wish to thank them for their philanthropy. Funding for the study was provided by the Department of Surgery Start-Up City of Hope.The authors would like to thank Byungwook Kim, Hannah Valencia, Seonah Kang, and Dr. Maria Hahn in our laboratory for technical support, and Dr. Supriya Deshpande for assistance with manuscript editing. The authors would also like to thank Betty Chang in the Small Animal Imaging Core; Kofi Poku, Junie Chea, and Nicole Bowles in the Radiopharmacy Core; and Drs. Aimin Li and Zhirong Yin in the Pathology Core of the City of Hope for supporting the work. The rights to CF33-hNIS-antiPDL1 (HOV3) are licensed to Imugene, Sydney, Australia.

AUTHOR CONTRIBUTIONS

Z.Z., Y.W., and Y.F. conceived and designed the experiments. Z.Z., A.Y., S.C., A.K.P., S.-I.K., T.O., and J.L. performed the experiments

Table 1. Mouse body weight in grams and clinical status

			Days post-tumor implantation																	
Treatment	Gender	Mouse ID	14	21	28	35	42	49	56	62	70	77	84	91	97	105	112	119	126	137
PBS	female	703	30	27[a]	26[a]	24[a]														
	male	712	36																	
	male	724	32	35	34	35	39													
	male	725	35	33	29	27[a]														
IT 3×10^5 days 1, 3, and 5	male	710	33	35	35	39	40	35	36	34	31	32	31							
	male	711	34	34	32	33	28													
	male	714	37	38	38	38	40	38	38	38	38	39	37	37	38	38	39	39	38	36
	male	715	33	33	31	29	30[a]													
	male	718	36	30																
	male	729	36	35	37	37	37													
	male	732	33	32	34	34	35	33	35	36	34	35	35	35	35	36	36	36	35	35
	female	702	24	25	26	25	25	22												

[a]Jaundice.

and helped interpret the data. Z.Z., A.Y., S.G.W., Y.F., and Y.W. analyzed and interpreted the data. Y.W. and Y.F. secured the funding. Z.Z., A.Y., and Y.W. drafted the manuscript. All of the authors edited and approved the final manuscript.

DECLARATION OF INTEREST

Y.F. is a paid scientific consultant for Medtronics, Johnson & Johnson, and Imugene, and receives royalties for inventions from Merck and from Imugene. All of the other authors declare no competing interests.

REFERENCES

1. Sung, H., Ferlay, J., Siegel, R.L., Laversanne, M., Soerjomataram, I., Jemal, A., and Bray, F. (2021). Global cancer statistics 2020: GLOBOCAN estimates of incidence and mortality worldwide for 36 cancers in 185 countries. CA Cancer J. Clin. *71*, 209–249.
2. Li, D., Xie, K., Wolff, R., and Abbruzzese, J.L. (2004). Pancreatic cancer. Lancet *363*, 1049–1057.
3. Werner, J., Combs, S.E., Springfeld, C., Hartwig, W., Hackert, T., and Buchler, M.W. (2013). Advanced-stage pancreatic cancer: therapy options. Nat. Rev. Clin. Oncol. *10*, 323–333.
4. Manji, G.A., Olive, K.P., Saenger, Y.M., and Oberstein, P. (2017). Current and emerging therapies in metastatic pancreatic cancer. Clin. Cancer Res. *23*, 1670–1678.
5. Teague, A., Lim, K.H., and Wang-Gillam, A. (2015). Advanced pancreatic adenocarcinoma: a review of current treatment strategies and developing therapies. Ther. Adv. Med. Oncol. *7*, 68–84.
6. Conroy, T., Desseigne, F., Ychou, M., Bouche, O., Guimbaud, R., Becouarn, Y., Adenis, A., Raoul, J.L., Gourgou-Bourgade, S., de la Fouchardiere, C., et al. (2011). FOLFIRINOX versus gemcitabine for metastatic pancreatic cancer. N. Engl. J. Med. *364*, 1817–1825.
7. Von Hoff, D.D., Ervin, T., Arena, F.P., Chiorean, E.G., Infante, J., Moore, M., Seay, T., Tjulandin, S.A., Ma, W.W., Saleh, M.N., et al. (2013). Increased survival in pancreatic cancer with nab-paclitaxel plus gemcitabine. N. Engl. J. Med. *369*, 1691–1703.
8. Fan, J.Q., Wang, M.F., Chen, H.L., Shang, D., Das, J.K., and Song, J. (2020). Current advances and outlooks in immunotherapy for pancreatic ductal adenocarcinoma. Mol. Cancer *19*, 32.
9. Amin, S., Baine, M., Meza, J., Alam, M., and Lin, C. (2020). The impact of immunotherapy on the survival of pancreatic adenocarcinoma patients who received definitive surgery of the pancreatic tumor: a retrospective analysis of the National Cancer Database. Radiat. Oncol. *15*, 139.
10. Schizas, D., Charalampakis, N., Kole, C., Economopoulou, P., Koustas, E., Gkotsis, E., Ziogas, D., Psyrri, A., and Karamouzis, M.V. (2020). Immunotherapy for pancreatic cancer: a 2020 update. Cancer Treat. Rev. *86*, 102016.
11. Russell, L., Peng, K.W., Russell, S.J., and Diaz, R.M. (2019). Oncolytic viruses: priming time for cancer immunotherapy. BioDrugs *33*, 485–501.
12. Haddad, D., and Fong, Y. (2015). Molecular imaging of oncolytic viral therapy. Mol. Ther. Oncolytics *1*, 14007.
13. Dohán, O., De la Vieja, A., Paroder, V., Riedel, C., Artani, M., Reed, M., Ginter, C.S., and Carrasco, N. (2003). The sodium/iodide symporter (NIS): characterization, regulation, and medical significance. Endocr. Rev. *24*, 48–77.
14. Dwyer, R.M., Bergert, E.R., O'Connor, M.,K., Gendler, S.J., and Morris, J.C. (2005). In vivo radioiodide imaging and treatment of breast cancer xenografts after MUC1-driven expression of the sodium iodide symporter. Clin. Cancer Res. *11*, 1483–1489.
15. Haberkorn, U. (2001). Gene therapy with sodium/iodide symporter in hepatocarcinoma. Exp. Clin. Endocrinol. Diabetes *109*, 60–62.
16. La Perle, K.M.D., Shen, D., Buckwalter, T.L.F., Williams, B., Haynam, A., Hinkle, G., Pozderac, R., Capen, C.C., and Jhiang, S.M. (2002). In vivo expression and function of the sodium iodide symporter following gene transfer in the MATLyLu rat model of metastatic prostate cancer. Prostate *50*, 170–178.
17. Hakkarainen, T., Rajecki, M., Sarparanta, M., Tenhunen, M., Airaksinen, A.J., Desmond, R.A., Kairemo, K., and Hemminki, A. (2009). Targeted radiotherapy for prostate cancer with an oncolytic adenovirus coding for human sodium iodide symporter. Clin. Cancer Res. *15*, 5396–5403.
18. Warner, S.G., Kim, S.-I., Chaurasiya, S., O'Leary, M.P., Lu, J., Sivanandam, V., Woo, Y., Chen, N.G., and Fong, Y. (2019). A novel chimeric poxvirus encoding hNIS is tumor-tropic, imageable, and synergistic with radioiodine to sustain colon cancer regression. Mol. Ther. Oncolytics *13*, 82–92.
19. Woo, Y., Zhang, Z., Yang, A., Chaurasiya, S., Park, A.K., Lu, J., Kim, S.I., Warner, S.G., Von Hoff, D., and Fong, Y. (2020). Novel chimeric immuno-oncolytic virus CF33-hNIS-antiPDL1 for the treatment of pancreatic cancer. J. Am. Coll. Surg. *230*, 709–717.
20. Chaurasiya, S., Yang, A., Kang, S., Lu, J., Kim, S.I., Park, A.K., Sivanandam, V., Zhang, Z., Woo, Y., Warner, S.G., et al. (2020). Oncolytic poxvirus CF33-hNIS-ΔF14.5 favorably modulates tumor immune microenvironment and works synergistically with

anti-PD-L1 antibody in a triple-negative breast cancer model. Oncoimmunology *9*, 1729300.

21. Rajecki, M., Sarparanta, M., Hakkarainen, T., Tenhunen, M., Diaconu, I., Kuhmonen, V., Kairemo, K., Kanerva, A., Airaksinen, A.J., and Hemminki, A. (2012). SPECT/CT imaging of hNIS-expression after intravenous delivery of an oncolytic adenovirus and 131I. PLoS One *7*, e32871.

22. Haddad, D., Chen, C.H., Carlin, S., Silberhumer, G., Chen, N.G., Zhang, Q., Longo, V., Carpenter, S.G., Mittra, A., Carson, J., et al. (2012). Imaging characteristics, tissue distribution, and spread of a novel oncolytic vaccinia virus carrying the human sodium iodide symporter. PLoS One *7*, e41647.

23. Barton, K.N., Stricker, H., Brown, S.L., Elshaikh, M., Aref, I., Lu, M., Pegg, J., Zhang, Y., Karvelis, K.C., Siddiqui, F., et al. (2008). Phase I study of noninvasive imaging of adenovirus-mediated gene expression in the human prostate. Mol. Ther. *16*, 1761–1769.

24. Chen, N.G., Yu, Y.A., Zhang, Q., and Szalay, A.A. (2011). Replication efficiency of oncolytic vaccinia virus in cell cultures prognosticates the virulence and antitumor efficacy in mice. J. Transl. Med. *9*, 164.

25. Jun, K.H., Gholami, S., Song, T.J., Au, J., Haddad, D., Carson, J., Chen, C.H., Mojica, K., Zanzonico, P., Chen, N.G., et al. (2014). A novel oncolytic viral therapy and imaging technique for gastric cancer using a genetically engineered vaccinia virus carrying the human sodium iodide symporter. J. Exp. Clin. Cancer Res. *33*, 2.

26. Chaurasiya, S., Chen, N.G., Lu, J., Martin, N., Shen, Y., Kim, S.I., Warner, S.G., Woo, Y., and Fong, Y. (2020). A chimeric poxvirus with J2R (thymidine kinase) deletion shows safety and anti-tumor activity in lung cancer models. Cancer Gene Ther. *27*, 125–135.

27. O'Leary, M.P., Choi, A.H., Kim, S.I., Chaurasiya, S., Lu, J., Park, A.K., Woo, Y., Warner, S.G., Fong, Y., and Chen, N.G. (2018). Novel oncolytic chimeric orthopoxvirus causes regression of pancreatic cancer xenografts and exhibits abscopal effect at a single low dose. J. Transl. Med. *16*, 110.

28. Choi, A.H., O'Leary, M.P., Lu, J., Kim, S.I., Fong, Y., and Chen, N.G. (2018). Endogenous Akt activity promotes virus entry and predicts efficacy of novel chimeric orthopoxvirus in triple-negative breast cancer. Mol. Ther. Oncolytics *9*, 22–29.

29. Zhang, Z., Yang, A., Chaurasiya, S., Park, A.K., Lu, J., Kim, S.I., Warner, S.G., Yuan, Y.C., Liu, Z., Han, H., et al. (2021). CF33-hNIS-antiPDL1 virus primes pancreatic ductal adenocarcinoma for enhanced anti-PD-L1 therapy. Cancer Gene Ther. https://doi.org/10.1038/s41417-021-00350-4.

30. Li, L., Liu, S., Han, D., Tang, B., and Ma, J. (2020). Delivery and biosafety of oncolytic virotherapy. Front. Oncol. *10*, 475.

31. Priceman, S.J., Gerdts, E.A., Tilakawardane, D., Kennewick, K.T., Murad, J.P., Park, A.K., Jeang, B., Yamaguchi, Y., Yang, X., Urak, R., et al. (2018). Co-stimulatory signaling determines tumor antigen sensitivity and persistence of CAR T cells targeting PSCA+ metastatic prostate cancer. Oncoimmunology *7*, e1380764.

32. Loening, A.M., and Gambhir, S.S. (2003). AMIDE: a free software tool for multimodality medical image analysis. Mol. Imaging *2*, 131–137.